Saturation Effect in the Temperature Dependence of a Proton Recombination with a Photobase†

Boiko Cohen and Dan Huppert*

Raymond and Beverly Sackler Faculty of Exact Sciences, School of Chemistry, Tel Aviv University, Tel Aviv 69978, Israel

Received: May 21, 2001; In Final Form: September 18, 2001

The temperature dependence of the reaction of a proton recombination with a photobase is studied in glycerol−water mixtures. For this purpose, we used a strong photobase, 7-hydroxy-4-methyl coumarin (4CUOH). The experimental data are analyzed using the bimolecular irreversible Smoluchowski theory. At high temperatures, the proton recombination rate is almost temperature independent, whereas at low temperatures, the rate constant has strong temperature dependence. The unusual temperature dependence is explained using proton-tunneling theory, based on the Landau−Zener curve crossing formulation. The high-temperature behavior of the rate constant denotes the nonadiabatic limit, whereas the low-temperature behavior denotes the adiabatic limit. We used an approximate expression for the proton-transfer rate, which bridges the nonadiabatic and the solvent controlled adiabatic limit to fit the temperature dependence curve of the experimental proton-transfer rate constant.

Introduction

A large experimental and theoretical effort has been made over the past several decades in order to understand the dynamics of intramolecular and intermolecular proton transfer in the gas phase, in clusters, and in the condensed phase.[1−18]

Studies of excited-state proton transfer (ESPT), from either a photoacid to the solvent or the transfer of a proton from the solvent to a photobase in solution, are fundamental to the understanding of the nature of the reactions of acids and bases in solution. These studies were conducted either on a photoacid molecule, which dissociates upon excitation to produce an excited anion and a proton, or on a photobase molecule that recombines with an excess proton in solution.[19−22] Even though this subject has been studied for many years,[23,24] the exact nature of both ESPT reactions is still not completely clear, nor is the dual role played by the solvent molecule (1) as proton acceptor or proton donor and (2) as a solvating medium of both the reactant and the product.[11,25,26]

In recent papers,[27−30] we described our experimental results on an unusual temperature dependence of excited-state proton transfer from a super photoacid (5,8-dicyano-2-naphthol, DCN2) to methanol, ethanol, propanol, diols, and glycerol. In all of the solvents at high temperatures, the rate of the proton transfer is almost temperature independent, whereas at low temperatures, the rate exhibits large temperature dependence. The values of the rate constant at low temperatures are similar to the inverse of the dielectric relaxation time. We proposed a simple stepwise model to describe and calculate the temperature dependence of the proton transfer to the solvent reaction. The model accounts for the large difference in the temperature dependence and the proton-transfer rate at high and low temperatures.

In the following paper, we extend the previous study of the temperature dependence dynamics of the transfer of a proton from a photoacid to the solvent[27−30] to a recombination of a photobase, 7-hydroxy-4-methyl coumarin (umbeliferon, 4CUOH), with a proton in glycerol−water mixtures. The photoacid and base properties of 4CUOH have been studied in various solvents in the past.[31−35]

Coumarin dyes are widely distributed in nature, and some of the derivatives are of great importance in chemistry, biochemistry, and medicine. Chen[36] indicated that 4CUOH is a useful indicator for following the pH change induced in the carbonic anhydrase catalyzed hydration of CO_2. Many coumarins are naturally fluorescent. In the ground state, hydroxy coumarins in aqueous solution have mild acid−base properties, $pK_a \sim 7$. In the excited state, they are much stronger acids−photoacids, $\Delta pK^* = (pK_a - pK_a^*) \approx 7$. 4CUOH shows dual photoreactivity in the excited state. In its neutral form, ROH*, it can transfer a proton to protic solvents. In water, the proton-transfer rate constant is large, $k_d \sim (20\ \text{ps})^{-1}$. In monols and glycerol, it is at least 3 orders of magnitude smaller, i.e., $k_d < 10^8\ \text{s}^{-1}$, i.e., smaller than the radiative rate. Hence, this process has a low quantum yield. The excited state 4CUOH can also react with the solvent, SOH, and abstract a proton, $ROH^* + SOH \rightarrow ROH_2^{+*} + SO^-$. It reacts much faster with excess protons in solution[32] to form ROH_2^{+*}. Thus, 4CUOH is also a strong photobase and can be used to study the recombination process of a proton with a photobase.

Experimental Methods and Data Analysis

7-hydroxy-4-methyl coumarin (4CUOH, Kodak, >99%, chemically pure) was dissolved in glycerol−water mixtures. Concentrated $HClO_4$ (Merck, Darmstadt 70% in aqueous solution) was added to the solution. Various glycerol−water mixtures with mole fractions of glycerol between 0.1 and 1, with acid concentrations between 0.1 and 1 M, were used. 4CUOH sample concentrations were between 2×10^{-4} and 5×10^{-4} M. In most of the experiments of this study, we used glycerol−water mixtures containing 60, 70, and 80 vol % of glycerol. All chemicals were used without further purification. Steady-state fluorescence spectra of the samples were recorded on an SLM-AMINCO-Bowman 2 luminescence spectrometer and corrected according to manufacturer specifications.

† Part of the special issue "Noboru Mataga Festschrift".

* To whom correspondence should be addressed. E-mail: huppert@tulip.tau.ac.il. Fax/phone: 972-3-6407012.

10.1021/jp011915i CCC: $22.00
Published on Web 02/07/2002

Time-resolved fluorescence was measured using the time-correlated single-photon counting (TCSPC) technique. As an excitation source, we used a cw mode-locked Nd:YAG-pumped dye laser (Coherent Nd:YAG Antares and a 702 dye laser) providing a high repetition rate (>1 MHz) of short pulses (2 ps at full width half-maximum, fwhm). The TCSPC detection system is based on a Hamamatsu 3809U, photomultiplier, Tennelec 864 TAC, Tennelec 454 discriminator, and a personal computer-based multichannel analyzer (nucleus PCA-II). The overall instrument response was about 50 ps (fwhm). Measurements were taken over a 10 nm spectral width. The samples were irradiated with laser pulses at 310 nm.

The temperature of the sample was controlled by placing the sample in an oven with thermal stability of approximately ±1 K.

Diffusive Model. The Smoluchowski theory is used to describe bimolecular irreversible diffusion-influenced reactions, in the pseudounimolecular limit, when one reactant (say, B) is in excess.[37] The initial decay of A is faster than at long times, because of the excess of B molecules at close proximity to A. As this density approaches its steady-state limit, the reaction becomes exponential, with a diffusion-control rate coefficient, k_D. Recently, we showed[38] that the theory fits nonexponential dynamics, observed in photoacid−base reactions.

The reaction of accepting an excess proton from the solvent by the excited 4CUOH molecule (ROH*), ROH* + $SOH_2^+ \rightarrow$ $ROH^+{}_2$* + SOH, can be described by a diffusive model. According to the Smoluchowski theory,[37] the survival probability of the proton acceptor (here, ROH*), because of its irreversible reaction with a concentration $c = [B]$ of donors, is given by

$$S'(t) = \exp(-c\int_0^t k(t')\,dt') \tag{1}$$

where $k(t)$ is the time-dependent rate coefficient (or, reactive flux at contact) for the donor−acceptor pair

$$k(t) = k_{PT}p(a,t) \tag{2}$$

The pair (ROH*/H^+) density distribution, $p(r,t)$, is governed by a Smoluchowski equation

$$\partial p(r,t)/\partial t = Dr^{-2}\frac{\partial}{\partial r}r^2\frac{\partial}{\partial r}p(r,t) \tag{3}$$

with an initial homogeneous distribution and a "radiation" boundary condition at the contact distance ($r = a$), depicting the occurrence of irreversible recombination upon the binary collision.

$$4\pi Da^2\frac{\partial}{\partial r}p(r,t)|_{r=a} = k_{PT}p(a,t) \tag{4}$$

For this particular case, of no potential between the reacting particles, it is possible to solve the DSE analytically. Collins and Kimball[39] found an exact expression for the time dependent rate constant:

$$k(t) = \frac{4\pi Dak_{PT}}{k_{PT}+4\pi Da}\left\{1+\frac{k_{PT}}{4\pi Da}e^{\gamma^2 Dt}\,\mathrm{erfc}[(\gamma^2 Dt)^{1/2}]\right\} \tag{5}$$

γ is given by

$$\gamma = a^{-1}\left(1+\frac{k_{PT}}{4\pi Da}\right) \tag{6}$$

erfc is the complementary error function. k_{PT} is the rate constant of the reaction at contact.

The survival probability of ROH* with finite lifetime τ_f, surrounded by an equilibrium distribution of excess protons with initial condition $S(0) = 1$, is

$$S(t) = \exp(-t/\tau_f - c\int_0^t k(t')\,dt') \tag{7}$$

where c is the concentration of the excess proton, $k(t)$ is the time dependent rate constant, given either by the numerical solution[40] or by eq 5,[39] and τ_f is the effective ROH* lifetime.

We solved eq 3 numerically, using a user-friendly Windows application for spherically symmetric diffusion problems (SSDP, ver. 2.61).[40] There are several input parameters for this model. a is taken as 7 Å, the value suggested by Weller.[41] k_{PT} is the bimolecular rate coefficient which, for 4CUOH in 60 vol % glycerol−water solution at room temperature, we find in this study to be $\sim 6 \times 10^{10}$ M^{-1} s^{-1}. These parameters did not vary with the acid concentration. The diffusion constant for the reaction is the mutual diffusion constant $D = D_{H^+} + D_{ROH^*}$. Its values in glycerol−water mixtures at all temperatures are unknown but could be evaluated up to a certain degree of confidence.

For 4CUOH, we estimate D from the viscosity according to the Stokes−Einstein relation, $D \propto 1/\eta$, and known literature values of D of similar compounds. For 2-naphthol in water (η = 1cp), Weller[41] suggested diffusion coefficients of 1.1×10^{-5} cm^2 s^{-1}. According to a more recent compilation,[42] the values for naphthol derivatives in water fall in the range of $0.55-0.65 \times 10^{-5}$ cm^2 s^{-1}. We calculated the value of D_{H^+} at room temperature for the studied water−glycerol mixtures from Erdey−Gruz conductivity measurements.[43]

The temperature dependence of the kinematic viscosity of glycerol−water mixtures was studied by Shankar and Kumar[44] in the temperature range 10−50 °C. They fit the viscosity data by an empirical correlation

$$(\ln \nu_m - \ln \nu_w)/(\ln \nu_g - \ln \nu_w) = x_g[1+(1-x_g)]\{a+bx_g+cx_g^2\} \tag{8}$$

where ν_w, ν_g, and ν_m are the kinematic viscosities of water, glycerol and the mixtures, respectively, and x_g is the mass fraction of glycerol in the mixtures. The empirical constants a, b, and c depend on temperature and are given in ref 44. The viscosities, as a function of temperature of neat water and glycerol, were taken from refs 45 and 46, respectively. For water above 100 °C, we extrapolate the values from a polynomial fit. The calculated viscosities of the glycerol−water mixtures as a function of temperature are shown in Figure 1a. For ions in solution, the diffusion constant can be calculated via the Stokes−Einstein relation from the viscosity data. Protons in aqueous solution and in alcohols have excess proton conductivity and diffusivity because of the prototropic mechanism.[43] The Walden product for protons $\eta\Lambda$ is not constant in water−glycerol mixtures,[43] and hence, the proton conductivity is not expected to follow the same temperature dependence of the viscosity. At low temperature, Erdey−Gruz[42] found for glycerol-water mixtures at all compositions that the activation energy of the conductivity is lower by ~25% from that of the viscosity. Thus, we expect that the temperature dependence of the proton conductivity will be significantly smaller from that of the viscosity. From the simulations of our data, we find that indeed the temperature dependence of the D is smaller from that of

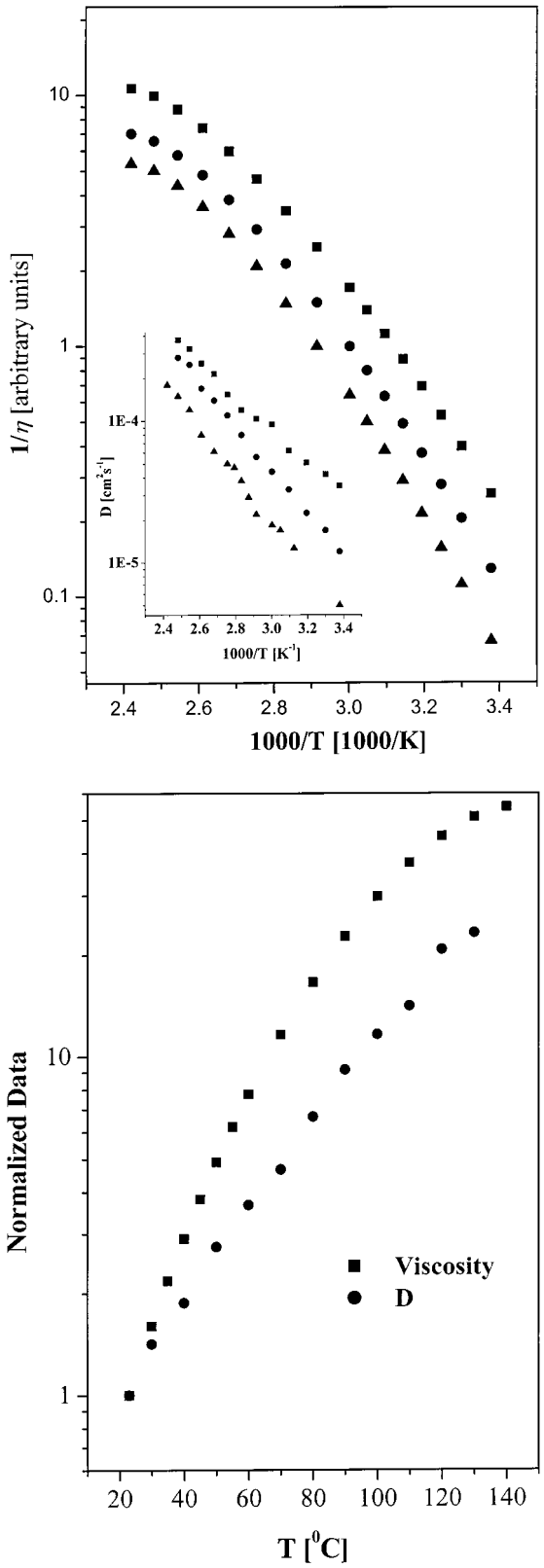

Figure 1. (a) Arrhenius plot of calculated $1/\eta$ of glycerol−water mixtures as a function of $1/T$; 60 vol % glycerol (■), 70 vol % glycerol (●), and 80 vol % glycerol (▲). Inset: The Arrhenius plot of the diffusion coefficients as used in the fit of the time-resolved emission data. (b) A comparison of D used in the fit and $1/\eta$ as a function of temperature for a 70% glycerol−water mixture.

viscosity. Figure 1b shows the comparison of D, used in the fit, and $1/\eta$ as a function of temperature for a 70% glycerol−water mixture.

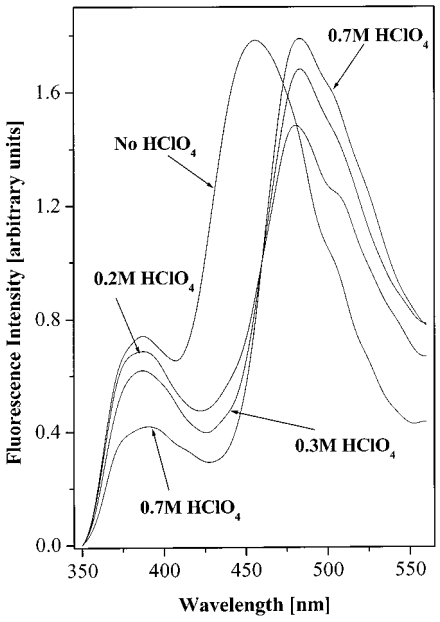

Figure 2. Steady-state emission spectra of 4CUOH at room temperature in a 60% glycerol−water mixture containing various concentrations of $HClO_4$.

Results

The excited-state protolytic reactions, involving the addition and subtraction of protons to the 4CUOH molecule, were studied by several groups in the past[31−33] and more recently by Bardez et al.[34] Upon excitation, both the acidity of the phenolic group and the basicity of the carbonyl group of 4CUOH are increased relative to the ground state. The steady-state emission of 4CUOH consists of three structureless broad bands, the maxima of which are at 380, 455, and 485 nm. The relative intensity of the emission bands depends on the solution pH and is assigned to the excited-state species, ROH* (380 nm, band maximum), RO^-* (455 nm), and ROH_2^+* (485 nm) forms.

The steady-state emission spectra of 4CUOH at room temperature in 60% glycerol−water mixture, containing various concentrations of $HClO_4$, are shown in Figure 2. As the acid concentration increases, the intensity of the ROH band at 380 nm decreases and the ROH_2^+ band intensity increases. The isoemissive point is at 460 nm, indicating that the ROH* + H^+ $\rightleftarrows$ ROH_2^+* process takes place in the excited state. The proton-transfer reaction ROH* $\rightarrow$ RO^-* + H^+ is slower than the photobase reaction when the HClO4 concentration is larger than 0.1 M. In 60% glycerol−water mixtures containing 1.0 M $HClO_4$, about 95% of the ROH* is consumed by the photobase reaction with an excess proton. At low acid concentration (0.25 M $HClO_4$), the parallel competitive reaction to produce RO^-* is quite effective and the RO^-* concentration increases to about 20%.

Figure 3 shows the time-resolved emission measured at 370 nm at several temperatures in the range of 294−403 K of an 80 vol % of glycerol−water mixture containing 0.29 M $HClO_4$. At all studied temperatures, the fluorescence decay was non-exponential, indicating that the reaction rate constant at contact, k_{PT}, is larger than the diffusion rate constant, k_D. At low temperatures, the average emission decay is long, indicating that the proton recombination reaction, as well as the diffusion rates, are relatively slow in the nanosecond range. The decay rates at high temperatures are faster, in the hundreds of picoseconds.

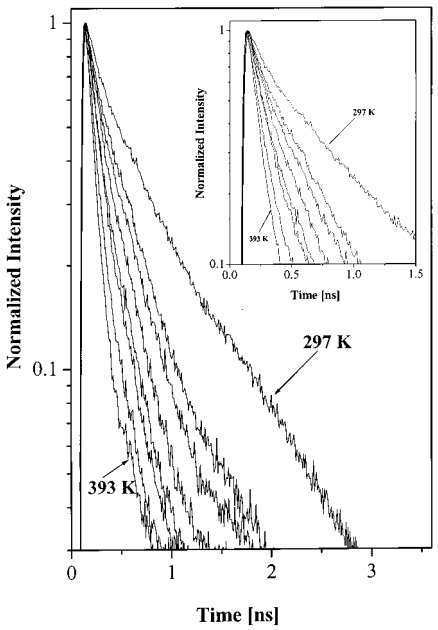

Figure 3. Time-resolved emission of 4CUOH, at 370 nm and at several temperatures in the range of 294−403 K, of an 80% glycerol−water mixture containing 0.29 M $HClO_4$. Top to bottom: 297, 313, 333, 343, 353, 373, 383, and 393 K.

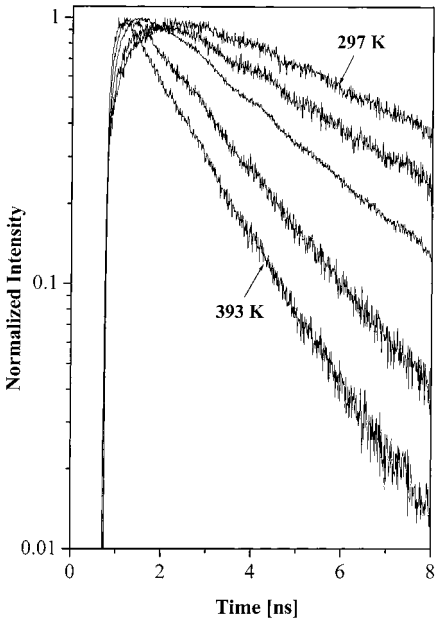

Figure 4. Time-resolved emission of the ROH_2^+ band of 4CUOH, measured at 530 nm at several temperatures. Top to bottom: 297, 313, 333, 373, and 393 K.

Figure 4 shows the time-resolved emission of the ROH_2^+ band measured at 530 nm at several temperatures. Each curve has a growth period followed by a relatively long exponential decay. For a particular temperature, the growth time fits the decay time of the emission of the ROH* species measured at 370 nm. At high temperatures, the rise time is much shorter than at room temperature, corresponding to a faster recombination reaction rate.

Figure 5 shows a calculated fit, using the Smoluchowski theory, to the experimental results of the time-resolved emission, measured at 370 nm, of 0.29 M $HClO_4$ 60% glycerol−water mixture at various temperatures. In the present analysis, the model parameters are a, the contact radius, k_{PT}, and $k_D = 4\pi DaN'$, where $N' = N_A/1000$ and N_A is Avogadro's number.

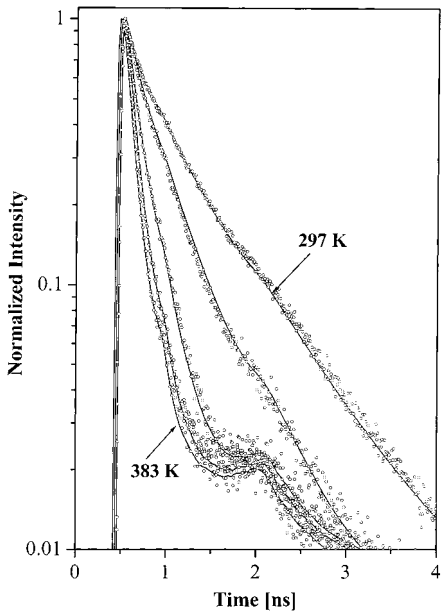

Figure 5. Calculated fit (solid line) to the time-resolved emission results (dots), measured at 370 nm, using the Smoluchowski theory. Top to bottom: 297, 313, 343, 363, and 383 K.

Following Weller, we take a as 7 Å. This leaves us with only two parameters that were adjusted to fit the data: k_{PT} and D. The diffusion influenced chemical reaction formalism separates the diffusion rate k_D from the "true" reaction rate constant, k_{PT}. k_D depends linearly on the value of the contact radius a. We used $a = 7$ Å, the same value suggested by Weller. We checked the influence of the value of a on the quality of the fit of the model to the experimental results and the value of k_{PT} extracted from the fit. We got good fits to the experimental results. When we change a from 7 to 5 Å, $D = 2.1 \times 10^{-4}$ cm^2 s^{-1} ($T = 373$ K, 60% glycerol−water mixture, 0.29 M $HClO_4$), k_{PT} changes from 5.9×10^{10} ($a = 7$ Å) to 5.5×10^{10} at $a = 5$ Å (7% of change). We believe that such a small change in the value of k_{PT} does not affect the temperature dependence of k_{PT}, which is the essence of this paper. The determination of the temperature dependence of the proton-transfer rate, k_{PT}, is the main goal of this study. The dynamics of the process is affected by the transport of the excess proton toward the 4CUOH molecule, which makes it difficult to obtain k_{PT}. The relevant parameters for the fit are given in Table 1.

Figure 6 parts a and b shows the time-resolved emission measured at 370 nm of 0.29 and 0.55 M $HClO_4$ 60% water−glycerol mixtures along with the model fit (solid line) at two temperatures, 298 (6a) and 373 K (6b). It can be seen that at a particular temperature we are able to get a good fit by changing only the acid concentration and keeping all of the other parameters constant.

The nonexponentiality of the decay curves enables us to differentiate the contribution of $k_{PT}(T)$ and $k_D(T)$ to the dynamics. The initial decay rate is determined by k_{PT}, and the long time behavior is determined by $k(\infty) = k_D k_{PT}/(k_D + k_{PT})$. When $k_{PT} > k_D$, which is the case for the low and medium-temperature data, $k(\infty) \cong k_D$. In such conditions, the decay curves are nonexponential, the proton-transfer rate determines the initial fast decay, and the value of D determines the long time behavior of the decay curve.

We conducted time-resolved emission measurements at various wavelengths in the spectral region 360−550 nm.

TABLE 1: Relevant Parameters for the Proton Transfer Reaction of 4CUOH in water-glycerol binary mixtures

$\tau_{ROH} = 2.1$ ns; $\tau_{RO^-} = 1.5$ ns; $\tau_{ROH_2^+} = 5$ ns[a]							
	60% glycerol		70% glycerol			80% glycerol	
T [K]	$10^5 D$[b] [$cm^2 s^{-1}$]	$10^{-10} k_{PT}$[c] [$M^{-1} s^{-1}$]	$10^5 D$ [$cm^2 s^{-1}$]	$10^{-10} k_{PT}$ [$M^{-1} s^{-1}$]	T [K]	$10^5 D$ [$cm^2 s^{-1}$]	$10^{-10} k_{PT}$ [$M^{-1} s^{-1}$]
296	3.5	2.14	1.2	1.35	298	0.5	0.98
303	4.3	2.63	1.7	1.69	320	1.27	1.80
313	5.6	3.20	2.3	2.14	323	1.7	1.99
323	7.3	3.57	3.3	2.44	328	1.85	2.22
333	9.5	4.14	4.4	3.10	333	2.2	2.56
343	9.7	4.89	5.6	3.38	343	2.9	2.86
353	10	5.34	8.0	3.94	348	3.8	3.12
363	15	5.64	11.0	4.13	353	4.7	3.38
373	21	5.90	14.0	4.58	358	5.0	3.57
383	25	6.02	17.0	4.77	363	6.1	3.80
393	32	6.20	25.0	4.88	373	8.0	3.91
403	37	6.32	28.0	4.96	383	12.0	4.06
					393	15.0	4.17
					403	18.0	4.25

[a] The excited-state lifetime of the ROH* form is measured in trifluorethanol where the proton-transfer reaction does not take place. [b] $D = D_{H^+} + D_{ROH^*}$, extracted from the best fit to the experimental data using Collins−Kimball equation (eq 5). [c] k_{PT} extracted from the best fit to the experimental data using Collins−Kimball equation (eq 5).

According to the irreversible diffusion model equations (eqs 1−7), the fluorescence intensity at a certain wavelength, ν, and time t, is given by a superposition of two contributions:

$$I(\nu,t) \propto S(t)g(\nu) + (1 - S(t))g'(\nu). \qquad (9)$$

$S(t)$ is the survival probability of ROH* and $1 - S(t)$ is the survival probability of ROH_2^+*. $g(\nu)$ and $g'(\nu)$ are the fluorescence line shapes of the ROH* and ROH_2^+*, respectively. The spectra were constructed from 18 time-resolved measurements at different wavelengths. Figure 7 shows the time-resolved spectra of 4CUOH 60% glycerol−water mixture containing 1.0 M $HClO_4$ at four times (10, 20, 100, 200, and 400 ps). The model calculation (eq 9), shown as solid line, fits nicely to the experimental data (points). The ROH* emission band intensity decreases with time, and the ROH_2^+* emission band increases with time.

Discussion

In the following section, we briefly describe the theory of proton transfer. This is followed by a description of our stepwise model accounting for the temperature dependence of the proton-transfer rate. Finally, the correlation of our model of proton transfer with the theory will be presented.

Kuznetsov and his colleagues[47] developed the model for nonadiabatic proton transfer, which is very similar in its treatment of the involvement of solvent to the model for nonadiabatic electron transfer. The fundamental assumption is that, when a barrier is encountered in the proton-transfer coordinate, the proton tunnels through the barrier, thus leading to a nonadiabatic process. In the Kuznetsov model,[47] when the polar solvent is equilibrated to the reactant, the proton will not be transferred because of an energy mismatch in the reactant and product states. Upon a solvent fluctuation, the energy of the reactant and product states becomes equal, and it is in this solvent configuration that the proton tunnels from one side of the well to the other. Finally, upon solvent relaxation, the product state is formed.

If the pretunneling and posttunneling configurations are regarded as real transient intermediates, the process for a photobase to recombine with a proton can be described by a set of chemical equations:[48]

$$\begin{aligned} B + {}^+H_2OS_A + S_R &\underset{k_{-1}}{\overset{k_1}{\rightleftharpoons}} B\cdot{}^+H_2OS_A + S_{\neq} \\ B\cdot{}^+H_2OS_A + S_{\neq} &\underset{k_{-2}}{\overset{k_2}{\rightleftharpoons}} BH^+\cdot HOS_A + S_{\neq} \\ BH^+\cdot HOS_A + S_{\neq} &\xrightarrow{k_3} BH^+ + HOS_A + S_p \end{aligned} \qquad (10)$$

where BH^+ is the protonated photobase, ${}^+H_2OS_A$ is a single protonated solvent molecule (the acid) from which the proton is transferred, S_R is the solvent configuration for stabilizing the reactants, and S_p is the solvent configuration of the products. $S_{\neq}$ is the solvent configuration to equally stabilize $B\cdot{}^+H_2OS_A$ and $BH^+\cdot HOS_A$.

Kuznetsov[47] and later on Borgis and Hynes[8] addressed the important issue of low-frequency vibrations in promoting proton transfer. One important difference between electron transfer and proton transfer is the extreme sensitivity of the proton tunneling matrix element to distance. Borgis and Hynes[8] derived the nonadiabatic rate constant, k. It was similar to that of Kuznetsov and co-workers,[47] but the tunneling term is significantly modified. The tunneling term strongly depends on a promoting vibration, Q.

Qualitative Model for the Temperature Dependence of Excited-State Proton-Transfer Reactions. The main findings of the experiments are as follows: (1) 4CUOH recombines with excess protons in the excited state in protic solvents. (2) In glycerol−water mixtures, at relatively low temperatures, the temperature dependence of the recombination rate constant follows $1/\tau_D$ where τ_D is the slow component of the dielectric relaxation. (3) In contrast to the low temperature behavior, at relatively high temperatures, the proton-transfer rate constant is almost temperature independent. (4) Similarly, we find the temperature dependence for the transfer of a proton from photoacids to protic solvents.[27−30]

Previously we used a qualitative model that accounts for the unusual temperature dependence of the proton transfer from a photoacid to the solvent.[27−30] The proton-transfer reaction

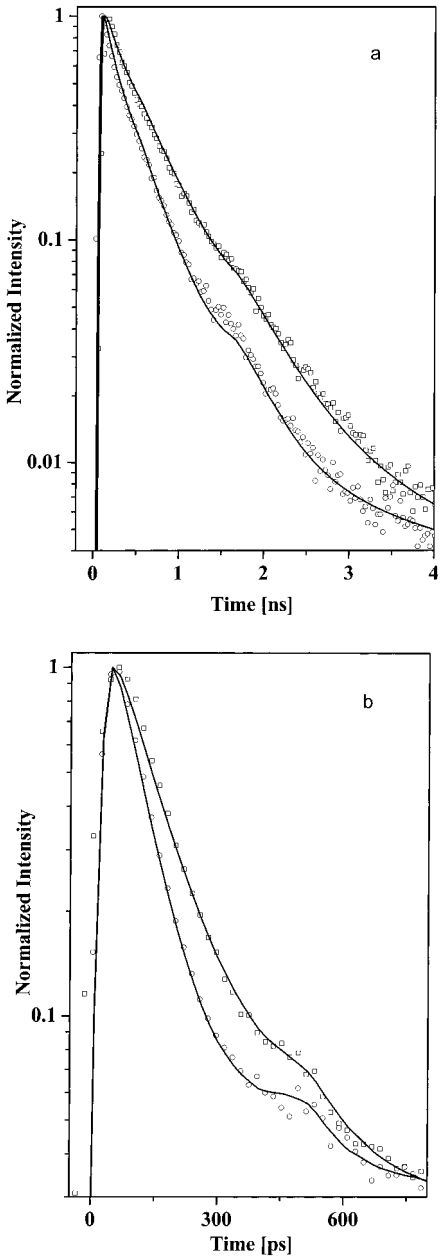

Figure 6. Experimental and DSE fit of the time-resolved emission of 4CUOH in 60% glycerol−water mixture measured at 370 nm at 0.25 and 0.55 M $HClO_4$. (a) $T = 298$ K and (b) $T = 373$ K.

depends on two coordinates. The first coordinate depends on a generalized solvent configuration. The solvent coordinate characteristic time is within the range of the dielectric relaxation time, τ_D, and the longitudinal relaxation, $\tau_L = \epsilon_0/\epsilon_s\ \tau_D$. The second coordinate is the actual proton translational motion (tunneling) along the reaction path, between the two oxygen atoms in this case.

The model restricts the proton transfer process to be stepwise. The proton moves to or from the adjacent hydrogen bonded solvent molecule only when the solvent configuration brings the system to the crossing point according to the Kuznetsov model.[47] This model excludes parallel routes for the ESPT in which many solvent configurations permit the reaction to take place with a distribution of reaction rates. In the stepwise model, the overall proton-transfer time is the sum of two times, $\tau = \tau_1 + \tau_2$, where τ_1 is the characteristic time for the solvent reorganization and τ_2 is the time for the proton to pass to the

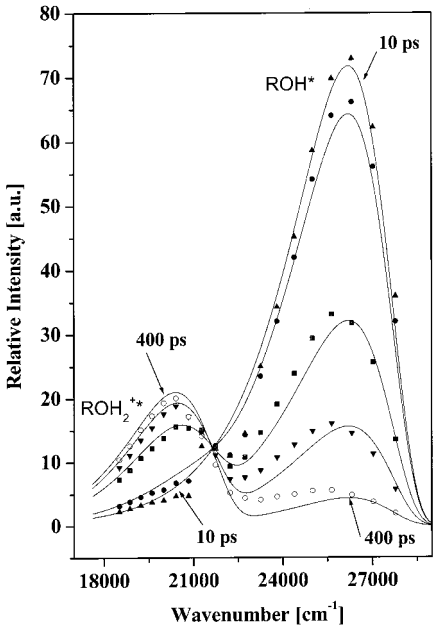

Figure 7. Time-resolved spectra of 4CUOH in 60% glycerol-water mixture containing 1.0 M $HClO_4$ measured at room temperature; experimental data: ▲, 10 ps; ●, 40 ps; ■, 100 ps; ▼, 200 ps; and ○, 400 ps; solid lines, model fit using eq 9 (see text).

acceptor. The overall rate constant, $k_{PT}(T)$, at a given T is

$$k_{PT}(T) = \frac{k_H(T)k_S(T)}{k_H(T) + k_S(T)} \tag{11}$$

where k_S is the solvent coordinate rate constant and k_H is the proton coordinate rate constant.

Equation 11 provides the overall excited-state proton-transfer rate constant along the lines of a stepwise process similar to the processes mentioned above. As a solvent coordinate rate constant, we use $k_S(T) = b(1/\tau_D)$, where b is an adjustable empirical factor determined from the computer fit of the experimental data. From our previous studies on ESPT of photoacids, we found that the empirical factor, b, lies between 0.65 and 4. For the alcohols, τ_L is usually smaller than τ_D by a factor of 2−6. Thus, the solvent characteristic time, $\tau_S = 1/k_S(T)$, for monols lies between the dielectric relaxation and the longitudinal time, $\tau_L < \tau_S < \tau_D$. Pines and co-workers[7,49] correlated the value of the proton dissociation rate k_d of many photoacids with their pK_a^* value. They used a procedure published by Agmon and Levine.[50] From the data analysis, they found $k_d^0 = 3 \times 10^{11}\ s^{-1}$ and $G_a^0 = 1.6$ kcal/mol.[7] This places the activationless limit of proton-transfer reactions between Debye relaxation time ($\tau_D \approx 8$ ps for water at 25 °C) and the longitudinal relaxation time $\tau_L = (\epsilon_\infty/\epsilon_s)\tau_D \approx (1 \pm 0.5)$ ps, where ϵ_∞ and ϵ_s are the dielectric constants of the solvent at high and low frequencies, respectively.

Robinson et al.[51] have suggested that moderately strong photoacids dissociate with an Arrhenius behavior given by $k_d = \tau_d^{-1} \exp(-G_a/k_BT)$, where τ_d is the collective dipole correlation time, $\tau_d \cong \tau_D$, and G_a is the activation free energy for dissociation, which is mainly determined by the change in the solvent entropy following the proton solvation by water.

The reaction rate constant, k_H, along the proton coordinate is expressed by the usual activated chemical reaction description given by eq 12. At high temperatures, the solvent relaxation is

fast and the rate determing step is the actual proton-transfer coordinate

$$k_H = k_H^0 \exp\left(-\frac{\Delta G^{\ddagger}}{RT}\right) \tag{12}$$

where k_H^0 is the preexponential factor determined by the fit to the experimental results and $\Delta G^{\ddagger}$ is the activation energy.

For photoacids, the activation energy, $\Delta G^{\ddagger}$, is determined from the excited-state acid equilibrium constant, K_a^*, and the structure reactivity relation. K_a^* is calculated from the rate parameters derived from the time-resolved emission at $\sim$ 320 K, assuming that $k_H \approx k_d$, according to

$$K_{a,chem}^* = 10^{27} k_d/(N_A k_a) \tag{13}$$

where N_A is Avogadro's number and k_d and k_a are the proton dissociation and recombination rate constants.[29] In this study, we deal with the reaction of a photobase with excess protons. The excited-state equilibrium constant is hard to determine because the dissociation rate of the bound proton $B^*H^+ \xrightarrow{k_d'} B^* + H^+$ is too slow to compete with the excited-state lifetimes, $k_d' < k_f$. Thus, we used $\Delta G^{\ddagger}$ as an adjustable parameter in our fitting procedure. We calculated the temperature dependence of the overall rate constant of the proton transfer from the solvent to the photobase using the above-mentioned procedure.

Qualitative Comparison of the Temperature Dependence of Proton Transfer with the Borgis−Hynes Theory. In this subsection, we compare our qualitative model, based on the experimental results, with the Borgis−Hynes theory for the proton transfer, which uses the Landau−Zener curve-crossing formalism.[8]

The reaction of a proton with a photobase can be described schematically:

$$B^*\cdots {}^+H_2OS_A \rightarrow BH^+{}^*\cdots HOS_A$$

The reactant is an intermolecular hydrogen-bonded complex between the photobase, B*, and a protonated solvent molecule, $^+H_2OS_A$, that serves as an acid, characterized by a hydrogen bond to the photobase and also to other solvent molecules. It was found that this hydrogen bond in protic solvents shifts the fluorescence band to the red by about 1000 cm^{-1}.[52] In water, this specific water molecule, $^+H_2OS_A$, has three hydrogen bonds to three water molecules. To form the product, $BH^+\cdots HOS_A$, in water, a hydrogen bond of HOS_A to an additional water molecule must be formed. Thus, relatively long-range reorganization of the hydrogen bond network takes place upon proton transfer to the photobase. Similar arguments of long-range rearrangement of the solvent can be said for proton transfer from a photoacid to the solvent. This complex, long-range rearrangement, to accommodate the product, is probably the reason for a slow generalized solvent configuration motion which corresponds to a low-frequency component in the solvent dielectric spectrum. Its time constant is close to the slow component of the dielectric relaxation time.

As mentioned above, our previous experiments indicate that the solvent fluctuation rate, to equalize the energies of reactant and product at the crossing point, is not of the order of 10^{13} s^{-1} but slower than 10^{12} s^{-1}. For monols, diols, and glycerol, it is very close to $1/\tau_D$, where τ_D is the slow component of the dielectric relaxation time.

Borgis and Hynes[8] derived an expression for the rate constant, k_{nm}, for the transition between the Q-vibrational state, n, in the reactant to the Q-vibrational state, m, in the product. They wrote an expression for k_{nm} in a transition state theory form. In particular, k_{nm} can be expressed as the average one-way flux in the solvent coordinate, through the crossing point S_{nm} of the two free energy curves for the n and m vibrational states, with the inclusion of the transmission coefficient, κ_{nm}, giving the probability of a successful curve crossing:

$$\kappa_{nm} = \langle \dot{S}\Theta(\dot{S})\delta(S - S_{nm})\kappa_{nm}(\dot{S}, S_{nm})\rangle_R \tag{14}$$

where S is the solvent coordinate, $\dot{S}$ is the solvent velocity, and $\Theta(\dot{S})$ is the positive velocity step function.

To find the appropriate nonadiabatic transmission coefficient factor, κ_{nm}, for use in this equation, Borgis and Hynes[8] used the general Landau−Zener (LZ) transmission coefficient, κ_{nm}, adapted for the present problem

$$\kappa_{nm} = [1 - 1/2 \exp(-\gamma_{nm})]^{-1}[1 - \exp(-\gamma_{nm})] \tag{15}$$

The LZ exponential factor, appropriate for a positive velocity approach to the crossing point, is

$$\gamma_{nm} = \frac{2\pi C_{nm}{}^2}{\hbar(\partial \Delta V_{nm}/\partial S)_{S_{nm}} \dot{S}} = \frac{2\pi C_{nm}{}^2}{\hbar k_S \dot{S}} \tag{16}$$

where ΔV_{nm} is the gap $V_m - V_n$ and includes multiple pass effects on the transition probability. (Note that $\kappa_{nm} \rightarrow 1$ is the adiabatic limit.) When $\gamma_{nm} \ll 1$, one obtains the nonadiabatic limit result

$$\kappa_{nm} = 2\gamma_{nm} \tag{17}$$

This leads to a state-to-state rate constant in the adiabatic limit

$$k_{nm} = \frac{2\pi}{\hbar} C_{nm}{}^2 \left[\left(\frac{\beta}{4E_S\pi}\right)^{1/2} e^{-\beta \Delta G^{\ddagger}_{nm}}\right] \tag{18}$$

in which $\Delta G_{nm}^{\ddagger}$ is the activation free energy

$$\Delta G_{nm}^{\ddagger} = \frac{1}{4E_S}(E_S + \Delta G + \Delta E_{nm})^2 \tag{19}$$

E_S is the solvent reorganization energy, and ΔG is the reaction free energy. γ_{nm} (see eq 16) depends on the potential surfaces curvature, $(\partial \Delta V_{nm}/\partial S)_{S_{nm}}$, on $C_{nm}{}^2$, and on $\dot{S}$. $C_{nm}{}^2$ depends on the Q intermolecular vibrational mode which is independent of T and S. The solvent velocity, $\dot{S}$, strongly depends on the temperature. In fact, $\dot{S}$ relates to the solvent relaxation. For photoacids, we found that $\dot{S} = b/\tau_D$, where τ_D is the solvent dielectric relaxation time and b is an empirical factor between 0.65 and 4. In all of the solvents used in our previous studies,[28−30] τ_D depends, nearly exponentially, on the temperature:

$$\gamma_{nm} \propto \tau_D(T)$$

$$\tau_D = \tau_D^0 \, e^{E_a/RT} \tag{20}$$

γ_{nm} assumes a low value at high temperature and a high value at low temperature. For the solvents used in this experiment, the value of γ_{nm} as a function of the temperature smoothly increases from a value close to 0, i.e., $\gamma \ll 1$ (the nonadiabatic limit, high temperature), to a value $\gamma \gg 1$ (the adiabatic limit, low temperature). In our previous study[30] on photoacids for ESPT in neat glycerol and diols, we used eq 15 to calculate κ_{nm} and $\gamma = 2\pi C_{nm}{}^2 \tau_S/\hbar k_s = 10^8 \tau_S$, where $\tau_S = \tau_D/b$. The

transmission coefficient, κ_{nm}, changes from close to zero at high temperatures (above 400 K) to close to 1 at low temperatures (below 325 K).

Borgis and Hynes[8] have also theoretically examined the situation of the Gadiabatic limit, which leads to the rate expression

$$k_{AD} = (\omega_s/2\pi)\exp(-\beta\Delta G^{\ddagger}) \qquad (21)$$

where ω_S is the solvent frequency and $\Delta G^{\ddagger}$ is the free energy of activation. In regular theoretical considerations, in the adiabatic limit, C_{nm}^2 is large, the gap is large, $\kappa_{nm} \approx 1$, and the reaction rate proceeds on an adiabatic potential surface. In our approach, C_{nm}^2 is an unknown and approximately constant over the studied temperature range, but $\dot{S}$, the solvent velocity, appearing in the denominator of γ (eq 16) depends exponentially on the temperature. Thus, at slow solvent velocity (low temperature), $\gamma \gg 1$ and $\kappa_{nm} \approx 1$, the proton-transfer reaction proceeds adiabatically; that is, the rate-limiting step is the solvent velocity. According to Borgis and Hynes[8] (eq 21), the preexponential factor will be of the order of 10^{13} s^{-1} or greater. This expression sets an upper limit of the fastest proton-transfer rate of about $(100\ fs)^{-1}$. Such a high rate has only been found this far in intramolecular proton transfer.[17,18] This rate is almost larger by a factor of 100 than the one found experimentally for the fastest intermolecular proton transfer.

Our expression for the stepwise model[27−30] (eq 11) is similar to the expression of Rips and Jortner[53] for the overall ET rate constant that bridges between the two extreme cases, the nonadiabatic and the adiabatic ET.

If we qualitatively use the Borgis−Hynes[8] formulas for nonadiabatic and adiabatic proton-transfer rate constants in a similar form as suggested by Rips and Jortner[53] for the overall expression of the electron-transfer rate constant (eq 3.38 in ref 50), we get

$$k_{PT}(T) = \frac{k_{PT}^{NA}(T)k_{PT}^{AD}(T)}{k_{PT}^{NA}(T) + k_{PT}^{AD}(T)} \qquad (22)$$

The formal expressions for k_{PT}^{NA} and k_{PT}^{AD} are given by eqs 18 and 21. k_{PT}^{NA} is qualitatively parallel to k_H in eqs 11 and 12. Accordingly, the prefactor, k_H^0, depends on the thermally average square coupling matrix. k_{PT}^{AD} is similar to k_S in eq 11. The time scale of the solvent control is slow and is close to τ_D. Using eq 22 to calculate $k_{PT}(T)$ as a function of the temperature results in qualitatively similar behavior to that in eq 11.

Estimation of the Dielectric Relaxation Time of the Studied Mixtures

In the process of calculation of the overall proton transfer by eq 11, we need to know the value of the solvent coordinate rate constant, $k_S(T) = b/\tau_D(T)$. $\tau_D(T)$ is the solvent dielectric relaxation time, and b is an empirical factor. We were unable to find in the literature the dielectric relaxation times of glycerol−water mixtures as a function of temperature.

The dielectric relaxation of neat glycerol was studied by Schneider et al.[54] The temperature dependence of both τ_D and the viscosity is almost the same in the temperature range of 20−100 °C. Above 100 °C, the temperature dependence of τ_D is slightly smaller.

The dielectric relaxation of water−alcohol mixtures was studied by Bertolini et al.[55] and Mashimo et al.[56] The longest dielectric relaxation time varies linearly with the mole fraction, x, of the mixture constituents for water−methanol and water−ethanol.

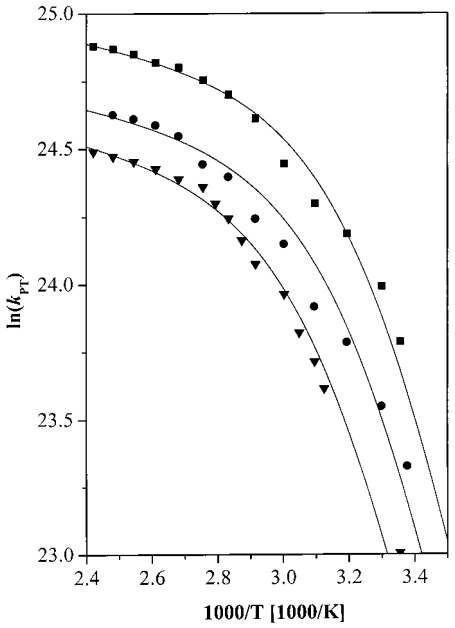

Figure 8. Arrhenius plot of the proton-transfer rate constant of 4CUOH in glycerol−water mixtures and 0.29 M $HClO_4$ as a function of $1/T$; 60 vol % glycerol (■), 70 vol % glycerol (●), and 80 vol % glycerol (▲). The calculated fit to the $\ln(k_{PT})$ using the stepwise model is shown as solid lines.

McDuffie et al.[57] measured the dielectric relaxation time of water−glycerol mixtures in the low-temperature range from −7.5 to −19.5 °C. The logarithm of the dielectric relaxation time of the mixtures obeys a linear relation with the mole fraction of the constituents. We estimate $\tau_D(T)$ for glycerol−water mixtures using the following procedure. We assume that τ_D, at low and medium-temperature ranges for the studied mixtures, follows the same dependence on x_g (the mass fraction) as the viscosity. We assume that Kumar's empirical correlation for the temperature dependence of the viscosity (eq 8) is also valid for τ_D

$$(\ln \tau_D^m - \ln \tau_D^w)/(\ln \tau_D^g - \ln \tau_D^w) = x_g[1 + (1 - x_g)]\{a + bx_g + cx_g^2\} \qquad (23)$$

where τ_D^m, τ_D^g, and τ_D^w are the dielectric relaxation times of the mixture, neat glycerol, and neat water, respectively. Thus, estimation of $\tau_D^m(T)$ from room temperature up to about 100 °C is evaluated. The next step is to estimate the temperature dependence of τ_D^m at high temperatures (T >100 °C). At these temperatures, $\tau_D^g(T)$ for neat glycerol deviates slightly from the viscosity temperature dependence. When the viscosity and τ_D^g are normalized, at $T_1 = 310$ K, the deviation at $T_2 = 400$ K of the ratio $\tau_D^g(T_2)/\tau_D^g(T_1)/\eta_D^g(T_2)/\eta_D^g(T_1)$ equals $^1/_2$. We therefore correct the estimate of $\tau_D^m(T > 370K)$ obtained from eq 23 by the above ratio.

Figure 8 shows the calculated fit (solid line) of $\ln(k_{PT})$ as a function of $1/T$ for three glycerol water mixtures, using the stepwise proton-transfer model, along with the experimental data. As can be seen, the model accounts for the change in the slope of the proton-transfer rate constant versus $1/T$. The relevant parameters for the fit are given in Table 2. As seen from the figure, the model calculation is in agreement with the measurements. The model accounts for the low and high-temperature

TABLE 2: Relevant Parameters for Model Calculations

glycerol[a]	glycerol[b]	$\Delta G^{\ddagger}$ [kJ/mol]	k_H^0[s^{-1}] 10^{-10}	k_H at 298 K [s^{-1}] 10^{-10}	k_S at 298 K [s^{-1}] 10^{-10}	τ_D[ps][c] at 298 K	b[d]
27	60%	2.0	11.5	5.2	2.2	173	3.8
37	70%	2.0	9.1	4.1	1.3	230	3.0
49	80%	2.0	8. 0	3.6	0.75	288	2.2

[a] Mole percent of glycerol. [b] Volume percent of glycerol. [c] τ_D is calculated by eq 23 (see text). [d] b is an empirical factor used in the determination of the proton-transfer rate at the low-temperature range ($k_S(T) = b/\tau_D$), see text).

regimes as well as the intermediate regime between them. There are three adjustable free parameters in the computer fits shown in Figure 8. These parameters are b, k_H^0, and $\Delta G^{\ddagger}$, where b is an empirical factor determined by $k_S(T) = b(1/\tau_D)$, k_H^0 is the preexponential in eq 12, and $\Delta G^{\ddagger}$ is the intrinsic activation energy. For a 60% glycerol−water mixture, the parameters are as follows: $k_H^0 = 1.15 \times 10^{11}$ s^{-1} and $k_S(T) = 3.8/\tau_D$. From Table 2, we find that the preexponential, k_H^0, depends on the glycerol mole fraction, and its value is about an order of magnitude larger than $1/\tau_D$ at room temperature. The empirical factor, b, ranges from 2.2 to 3.8, similar values to those we used for photoacids. We used $\Delta G^{\ddagger} = 2$ kJ/mol for the reaction of 4CUOH with excess proton in all three mixtures, similar to the value of $\Delta G^{\ddagger}$ we used for the proton transfer from DCN2.[30] The activation energies are small, and for the fit of the data, we used the same value for all solvent mixtures.

Summary

We studied, using time-resolved emission techniques, the temperature dependence of the reaction of an excess proton with a photobase. 4CUOH is used as the excited-state photobase. The experimental time-resolved fluorescence data are analyzed by the bimolecular irreversible diffusion-influenced Smoluchowski theory.

We have found that the proton recombination rate constant, k_{PT}, with excited 4CUOH in glycerol−water mixtures at relatively high temperatures is almost temperature independent, whereas at lower temperatures, the proton recombination rate is similar to the inverse of the dielectric relaxation time.

A two-coordinate stepwise model has been used to explain the temperature dependence of the reaction. Previously, we used the model to explain proton transfer to the solvent from a photoacid.[27−30] Our model can be qualitatively compared with the Borgis-Hynes proton transfer theory based on the Landau−Zener curve crossing formulation. The unusual temperature dependence of both the proton recombination with the photobase and the dissociation of a proton from a photoacid can be explained as a continuous transition from the nonadiabatic regime (the high-temperature limit) to the adiabatic regime (the low-temperature limit).

Acknowledgment. This work was supported by grant from the Binational U.S.−Israel Science Foundation (BSF) and the James-Franck German−Israel Program in Laser-Matter Interaction. We thank Tatiana Molotsky for her help in the construction of the time-resolved spectra.

References and Notes

(1) Knochenmuss, R. *Chem. Phys. Lett.* **1998**, *293*, 191.
(2) Hineman, M. F.; Brucker, G. A.; Kelley, D. F.; Bernstein, E. R. *J. Chem. Phys.* **1992**, *97*, 3341.
(3) Peters, K. S.; Cashin, A.; Timbers, P. *J. Am. Chem. Soc.* **2000**, *122*, 107.
(4) Syage, J. A. *J. Phys. Chem.* **1995**, *99*, 5772.
(5) Tsutsumi, K.; Shizuka, H. *Z. Phys. Chem* **1980**, *122*, 129.
(6) Prayer, C.; Gustavsson, T.; Tran-Thi, T.-H. *Fast Elementary Processes in Chemical and Biological Systems*; AIP: Woodbury, NY, 1996; Vol. 364, pp 333−339. Tran-Thi, T.-H.; Gustavsson, T.; Prayer, C.; Pommeret, S.; Hynes, J. T. *Chem. Phys. Lett.* **2000**, *329*, 421.
(7) Pines, E.; Tepper, D.; Magnes, B.-Z.; Pines, D.; Barak, T. *Ber. Buns. Phys. Chem.* **1998**, *102*, 504. Pines, E.; Pines, D.; Barak, T.; Magnes, B.-Z.; Tolbert, L. M.; Haubrich, J. E. *Ber. Buns. Phys. Chem.* **1998**, *102*, 511.
(8) Borgis, D.; Hynes, J. T. *J. Phys. Chem.* **1996**, *100*, 1118. Borgis, D. C.; Lee, S.; Hynes, J. T. *Chem. Phys. Lett.* **1989**, *162*, 19. Borgis, D.; Hynes, J. T. *J. Chem. Phys.* **1991**, *94*, 3619.
(9) Li, D.; Voth, G. A. *J. Phys. Chem.* **1991**, *95*, 10425. Lobaugh, J.; Voth, G. A. *J. Chem. Phys.* **1994**, *100*, 3039.
(10) Cukier, R. I.; Morillo, M. *J. Chem. Phys.* **1989**, *91*, 857. Morillo, M.; Cukier, R. I. *J. Chem. Phys.* **1990**, *92*, 4833.
(11) Ando, K.; Hynes, J. T. In *Structure, energetics and reactivity in aqueous solution*; Cramer, C. J., Truhlar, D. G., Eds.; ACS Books: Washington, DC, 1994.
(12) Douhal, A.; Lahmani, F.; Zewail, A. H. *Chem. Phys.* **1996**, *207*, 477
(13) Arnaut, L. G.; Formosinho, S. J. *J. Photochem. Photobiol. A* **1993**, *75*, 1. Arnaut, L. G., Formosinho, S. J. *J. Photochem. Photobiol. A* **1993**, *75*, 21.
(14) Mente, S.; Maroncelli, M. *J. Phys. Chem. A* **1998**, *102*, 3860.
(15) Bardez, E.; Devol, I.; Larrey, B.; Valeur, B. *J. Phys. Chem. B* **1997**, *101*, 7786. Bardez, E.; Fedorov, A.; Berberan-Santos, M. N.; Martinho, J. M. G. *J. Phys. Chem. A* **1999**, *103*, 4131. Bardez, E. *Isr. J. Chem.* **1999**, *39*, 319.
(16) Barbara, P. F.; Vonborcyzskowski, C.; Casalegno, R.; Corval, A.; Krzschi, C.; Romanowski, Y.; Trommsdoff, H. P. *Chem. Phys.* **1995**, *199*, 285.
(17) Chudoba, C.; Riedle, E.; Pfeiffer, M.; Elsaesser, T. *Chem. Phys. Lett.* **1996**, *263*, 622.
(18) Ernstig, N. P.; Kovalenko, S. A.; Senyushkina, T.; Saam, J.; Farztdinov, V. *J. Phys. Chem.* **2001**, *105*, 3443.
(19) Ireland, J. F.; Wyatt, P. A. H. *Adv. Phys. Org. Chem.* **1976**, *12*, 131.
(20) Huppert, D.; Gutman, M.; Kaufmann, K. J. In *Advances in Chemical Physics*; Jortner, J., Levine, R. D., Rice, S. A., Eds.; Wiley: New York, 1981; Vol. 47, p 681. Koswer, E.; Huppert, D. In *Annual Reviews of Physical Chemistry*; Strauss, H. L., Babcok, G. T., Moore, C. B., Eds.; (Annual Reviews Inc.: Palo Alto, CA, 1986; Vol. 37, p 122.
(21) Lee, J.; Robinson, G. W.; Webb, S. P.; Philips, L. A.; Clark, J. H. *J. Am. Chem. Soc.* **1986**, *108*, 6538.
(22) Gutman, M.; Nachliel, E. *Biochim. Biophys. Acta* **1990**, *391*, 1015.
(23) Förster, Th. *Z. Natuwiss.* **1949**, *36*, 186.
(24) Weller, A. *Prog. React. Kinet.* **1961**, *1*, 189.
(25) Kolodney, E.; Huppert, D. *J. Chem. Phys.* **1981**, *63*, 401.
(26) Agmon, N.; Huppert, D.; Masad, A.; Pines, E. *J. Phys. Chem.* **1991**, *96*, 952.
(27) Carmeli, I.; Huppert, D.; Tolbert, L. M.; Haubrich, J. E. *Chem. Phys. Lett.* **1996**, *260*, 109
(28) Poles, E.; Cohen, B.; Huppert, D. *Isr. J. Chem.* **1999**, *39* (3−4), 347.
(29) Cohen, B.; Huppert, D. *J. Phys. Chem. A* **2000**, *104*, 2663.
(30) Cohen, B.; Huppert, D. *J. Phys. Chem. A* **2001**, *105*, 2980.
(31) Shank, C. V.; Dienes, A.; Trozollo, A. M.; Mayer, J. A. *Appl. Phys. Lett.* **1970**, *10*, 405.
(32) Yakatan, G. J.; Juneau, R. J.; Schulman, S. G. *Ann. Chem.* **1972**, *44*, 1044.
(33) Bauer, P. K.; Kowalczyk, A. Z. *Naturforsch.* **1980**, *35a*, 946.
(34) Bardez, E.; Boutin, P.; Valeur, B. *Chem. Phys. Lett.* **1992**, *191*, 142.
(35) Huppert, D.; Cohen, B. *J. Phys. Chem. A* **2001**, *105*, 7157.
(36) Chen, R. F. *Anal. Lett.* **1968**, *1*, 423.
(37) Von Smoluchowski, M. *Ann. Phys.* **1915**, *48*, 1103.
(38) Cohen, B.; Huppert, D.; Agmon, N. *J. Am. Chem. Soc.* **2000**, *122*, 9838.
(39) Collins, F. C.; Kimball, G. E. *J. Colloid Sci.* **1949**, *4*, 425.
(40) Krissinel', E. B.; Agmon, N. *J. Comput. Chem.* **1996**, *17*, 1085.
(41) Weller, A. *Z. Elektrochem.* **1954**, *58*, 849. Weller, A. *Z. Phys. Chem. N. F.* **1958**, *17*, 224.
(42) Sharma, L. R.; Kalia, R. K. *J. Chem. Eng. Data* **1977**, *22*, 39.
(43) Erdey-Gruz, T.; Kugler, E. *Magyar Kemiai Folyoirat* (in Hungarian) **1968**, *74*, 135. Erdey-Gruz, T.; Lengyel, S. In *Modern Aspects of Electrochemistry*; Bockris, J. O'M., Conway, B. E., Eds.; Plenum: New York, 1964; Vol. 12, pp 1−40.
(44) Shankar, P. N.; Kumar, M. *Proc. R. Soc. London A* **1994**, *444*, 573.

(45) *Handbook of Chemistry and Physic*s, 66th ed; Weast, R. C., Astle, M. J., Eds; CRC Press: Boca Raton, FL, 1985.

(46) Yen-Ming Chen, Pearlstein, A. *J. Ind. Eng. Chem. Res.* **1987**, *26*, 1670.

(47) German, E. D.; Dogonadze, R. R.; Kuznetsov, A. M.; Levich, V. G.; Kharkats, Yu. I. *Elektrokhimiya* **1970**, *6*, 350. German, E. D.; Kuznetsov, A. M.; Dogonadze, R. R. *J. Chem. Soc., Faraday Trans. 2* **1980**, *76*, 1128. German, E. D.; Kuznetsov, A. M. *J. Chem. Soc., Faraday Trans. 1* **1981**, *77*, 397. German, E. D.; Kuznetsov, A. M. *J. Chem. Soc., Faraday Trans. 2* **1981**, *77*, 2203. Ulstrup, J. *Charge-Transfer Processes in Condensed Media*; Springer: Berlin, Germany, 1979.

(48) Kreevoy, M. M.; Kotchevar, A. T. *J. Am. Chem. Soc.* **1990**, *112*, 3579. Kotchevar, A. T.; Kreevoy, M. M. *J. Phys. Chem.* **1991**, *95*, 10345.

(49) Pines, E.; Fleming, G. R. *Chem. Phys. Lett.* **1994**, *183*, 393. Pines, E.; Magnes, B.; Lang, M. J.; Fleming, G. R. *Chem. Phys. Lett.* **1997**, *281*, 413.

(50) Agmon, N.; Levine, R. D. *Chem. Phys. Lett.* **1977**, *52*, 197. Agmon, N.; Levine, R. D. *Isr. J. Chem.* **1980**, *19*, 330.

(51) Robinson, G. W.; Thistlehwaite, P. J.; Lee, J. *J. Phys. Chem.* **1986**, *90*, 4224.

(52) Solntsev, K.; Huppert, D.; Agmon, N. *J. Phys. Chem. A* **1999**, *103*, 6984.

(53) Rips, I.; Jortner, J. *J. Chem. Phys.* **1987**, *87*, 2090.

(54) Schneider, U.; Lunkenheimer, P.; Brand, R.; Loidl, A. *J. Non-Cryst. Solids* **1998**, *173*, 235.

(55) Bertolini, D.; Cassettari, M.; Salvetti, G. *J. Chem. Phys.* **1983**, *78*, 365.

(56) Mashimo, S.; Kuwabara, S.; Yagihara, S.; Higasi, K. *J. Chem. Phys.* **1989**, *90*, 3292.

(57) McDuffie, G. E.; Quinn, R. G.; Litovitz, T. A. *J. Chem. Phys.* **1962**, *37*, 239.